Journal of Organometallic Chemistry, 272 (1984) 169–177
Elsevier Sequoia S.A., Lausanne – Printed in The Netherlands

PROTONATION AND PROTOLYSIS OF $[Fe_4(CO)_{12}(CCH_3)]^-$ *

P.L. BOGDAN, K.H. WHITMIRE **, J.W. KOLIS, D.F. SHRIVER,
Department of Chemistry, Northwestern University, Evanston, IL 60201 (U.S.A.)

and E.M. HOLT
Department of Chemistry, Oklahoma State University, Stillwater, OK 74078 (U.S.A.)

(Received February 1st, 1984)

Summary

The reaction of $[Fe_4(CO)_{12}(CCH_3)]^-$ with HSO_3CF_3 in CH_2Cl_2 solution yields the compound $HFe_4(CO)_{12}(CCH_3)$, which was characterized chemically, spectroscopically and by single crystal X-ray diffraction. This compound retains the approximately tetrahedral 4-iron framework characteristic of the parent anion and protonation appears to have occurred on an Fe–Fe bond. In neat HSO_3CF_3, infrared and NMR spectroscopic evidence indicates that another proton adds to the metal framework producing $[H_2Fe_4(CO)_{12}(CCH_3)]^+$. On long standing, this solution evolves CO, and H_2, and small amounts of CH_4 and C_2H_6. On the time scale of the experiments described here the latter two gases are obtained in an approximately 1/3 ratio. Deuterated acid leads to mixtures of the various isotopomers of CH_4 but the ethane is CD_3CH_3. Possible mechanisms for hydrocarbon production are discussed.

Introduction

The reaction of $[Fe_4(CO)_{13}]^{2-}$ with strong acids goes through an interesting series of transformations, which culminate in the production of CH_4 and oxidized iron species, eq. 1 [1–3]. One feature of this reaction which is relevant to the present work is the generation of a fairly stable cationic protonated metal carbonyl cluster, V, eq. 1. Initial protonation of the tetrahedral 4-iron array produces a 4-iron butterfly compound, II [4], and this open metal framework persists through the series of intermediate compounds from II through V.

* Dedicated with felicity to Professor Sei Otsuka.
** Present address: Rice University, Houston TX 77001 (U.S.A.).

0022-328X/84/$03.00

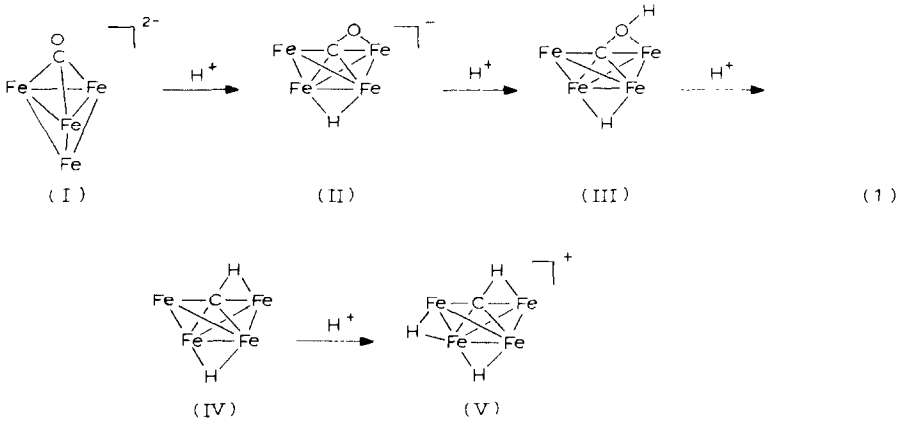

In the present research we have explored the reactions of $[Fe_4(CO)_{12}(CCH_3)]^-$ (VI) with strong acid. Again a stable cationic cluster is produced rapidly and hydrocarbon evolution is slow, but the details are very different from those outlined in eq. 1.

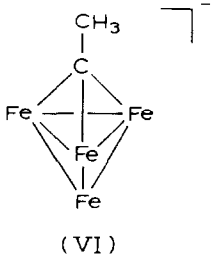

Experimental

General procedures. All reactions were carried out under anhydrous conditions using standard vacuum line and Schlenk techniques. Solvents were dried as follows: CH_2Cl_2 (reflux over P_2O_5), hexane (reflux over Na/benzophenone), HSO_3CF_3 (vacuum distilled in flame-dried glassware). $[PPN][Fe_4(CO)_{12}CCH_3]$ was prepared as previously described [5], and great care was taken to obtain a pure product free from $HFe_4(CO)_{12}(CH)$ (PPN = bistriphenylphosphinenitrogen(1 +)). Compounds suitable for ^{13}C NMR spectroscopy were obtained from $[PPN]_2[Fe_4(CO)_{13}]$ [6] which had been enriched by stirring in CH_2Cl_2 solution overnight under an atmosphere of 90% ^{13}CO.

IR spectra were obtained with a Perkin–Elmer 399 spectrometer, and NMR spectra on JEOL FX-90Q or FX-270 instruments. Mass spectra were determined on a Hewlett–Packard 5985, and analyzed by M. Andrews' program MASPAN. Elemental analyses were performed by Galbraith Laboratories.

Preparation of $HFe_4(CO)_{12}CCH_3$. To 0.20 g of $[PPN][Fe_4(CO)_{12}CCH_3]$ in 5 ml of CH_2Cl_2 0.04 ml of HSO_3CF_3 was added while stirring. After 15 min, the solvent was removed under vacuum. The residue was extracted with 25 ml of hexane and

filtered to remove a grey solid. Removal of hexane under vacuum resulted in a brown-black microcrystalline powder. Anal. Found: C, 24.98; H, 0.76; Fe, 39.45. $C_{14}H_4Fe_4O_{12}$ calcd.: C, 28.62; H, 0.69; Fe, 38.00%. (Carbon analyses are consistently low with these types of compounds.) Mass spectral analysis showed the parent ion at $m/e = 588$. Calculated spectrum for parent envelope: (m/e; intensity) 589, 15.23; 588, 59.56; 586, 14.97. Observed: 589, 18.46; 588, 63.07; 586, 18.46. IR ν(CO), toluene: 2080w, 2045vs, 2030s, 1978m cm^{-1}. ^1H NMR; toluene-d_8: δ 4.1 (CH_3), −20.3 (hydride) ppm. ^{13}C NMR; CD_2Cl_2: δ 359.2 (α-C), 212.5, 212.2, 209.6, 208.4, 207.3, 204.6 (CO) with relative intensities 1/1/16/3/2/1. Small crystals suitable for X-ray analysis were obtained by slow cooling of a concentrated hexane solution of the product.

Gas evolution reactions. To 6.0 ml of frozen HSO_3CF_3 a measured quantity of $[PPN][Fe_4(CO)_{12}CCH_3]$ was added. The flask was evacuated on a high-vacuum line, thawed, and stirred at room temperature for 7–14 days. For analysis, the flask was immersed in a Dry Ice/acetone bath, and volatiles were passed through a silica gel trap at −196 °C, which condensed CH_4 and less volatile gases. The hydrogen, which passed through the silica gel trap, was collected with a Toepler pump and measured in a gas buret. The condensible gases were separated, identified, and qualitatively measured by gas chromatography using a Spherocarb column and thermal conductivity detector.

NMR study in HSO_3CF_3. A 10 mm NMR tube was charged with 90 mg of $HFe_4(CO)_{12}CCH_3$, cooled to −196 °C, and HSO_3CF_3, 3 ml, was added under N_2 purge via an all-glass gas-tight syringe. The tube was sealed under vacuum, warmed to room temperature, and put in the spectrometer probe at −30 °C. ^1H NMR spectra were run with the HSO_3CF_3 signal at δ 11.13 ppm eliminated by double resonance techniques.

Structure determination. A crystal of $HFe_4(CO)_{12}(CCH_3)$ was sealed in a capillary and mounted on a Syntex P3 automated diffractometer. Unit cell dimensions (Table 1) were determined by least squares refinement of the best angular positions for fifteen independent reflections ($2\theta > 15°$) during normal alignment procedures using molybdenum radiation (λ 0.71069 Å). Data (4602 points) were collected at room temperature using a variable scan rate, a θ–2θ scan mode and a scan width of 1.2° below K_{α_1} and 1.2° above K_{β_2} to a maximum 2θ value of 116°. The background was measured on each side of the scan for a combined time equal to the total scan time. The intensities of three standard reflections were remeasured after every 97 reflections. Since the intensities of these reflections showed less than 8% variation, corrections for decomposition were deemed unnecessary. Data were corrected for Lorentz, polarization and background effects. After removal of redundant and space group forbidden data, 1502 reflections were considered observed [$I > 3.0\sigma(I)$]. The structure was solved from a Patterson synthesis to locate the heavy atoms. Successive least squares/difference Fourier cycles allowed location of the remainder of the nonhydrogen atoms. Refinement [7] of scale factor, positional and anisotropic thermal parameters for all nonhydrogen atoms was carried out to convergence. Hydrogen positional parameters could not be determined. The final cycle of refinement [function minimized $\Sigma(|F_o| - |F_c|)^2$] led to a final agreement factor, $R = 5.2\%$ [$R = (\Sigma||F_o| - |F_c||/|F_o|) \times 100$]. Anomalous dispersion corrections were made for Fe. Scattering factors were taken from Cromer and Mann [8]. Unit weights were used throughout.

TABLE 1

CRYSTAL DATA FOR $HFe_4(CO)_{12}(CCH_3)$

Formula	$C_{14}H_4Fe_4O_{12}$
Mol. wt.	587.52
a	8.977(3) Å
b	8.977(3) Å
c	41 485(16) Å
α	90.0 °
β	90.0 °
γ	120.0 °
V	2895 2(17) $Å^3$
$F(000)$	1728
μMo-K_α	30.09
λMo-K_α	0.71073 Å
D_{calc}	2.02 g cm^{-3}
Z	6
Obs. refl.	1502
R	5.2%
Space group	$P3_221$

Results and discussion

The starting material, $[Fe_4(CO)_{12}(CCH_3)]$ (VI) has a pseudo-tetrahedral structure, even though it is derived from a 4-iron butterfly carbide according to eq. 2 [5]. As previously described [6], this transformation can be readily understood in terms of the cluster valence electron (CVE) count [9], which is 62 in the butterfly starting material, but is reduced to 60 upon alkylation of the carbide ligand by a methyl carbocation. The 60 CVE count is appropriate for the tetrahedral ethylidyne cluster which results, and for the protonated product, $HFe_4(CO)_{12}(CCH_3)$, which is discussed below.

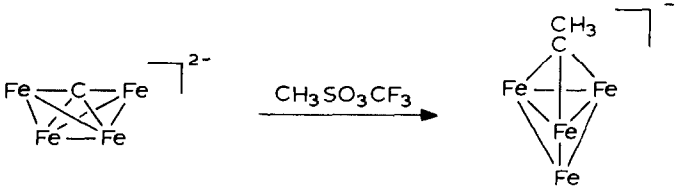

(VII) (VI) (2)

$HFe_4(CO)_{12}(CCH_3)$. The protonation of VI proceeds rapidly to produce a brown-black product, which may be contaminated with the methylidyne, IV, if impure starting materials are used. To avoid this impurity, which was highly undesirable for the gas evolution studies, pure carbide, VII, was used and adventitous sources of protons were excluded in the alkylation step, eq. 2. The resulting ethylidyne product, VI, was free from the methylidyne, IV, as judged by NMR spectroscopy.

The ^1H NMR spectrum of $HFe_4(CO)_{12}(CCH_3)$ in toluene-d_8 exhibits a methyl

resonance at δ 4.1 ppm and a high-field resonance at -20.3 ppm. The methyl resonance is very close to that of the parent monoanion, VI, δ 4.2 ppm, and the high field resonance is in a region characteristic of metal "hydrides". The X-ray crystal structure, Fig. 1, is consistent with this interpretation. The ^{13}C NMR spectrum, of a sample which had been enriched at the carbide and carbonyl atoms in the starting material, VII, displayed resonances in the range δ 205–210 ppm and a singlet at δ 359 ppm. The former is characteristic of terminal carbonyls and the latter is assigned to the α-carbon in the ethylidyne, which is close to that in the starting anion, δ 357 ppm [5]. The methyl group was not ^{13}C enriched and therefore was not observed.

The mass spectrum of this compound is characterized by a parent peak at *m/e* 588 with associated envelope for the related isotopic molecules. A series of similar envelopes is observed at mass 28 intervals corresponding to the sequential loss of CO ligands. The theoretical intensity distributions of the various isotopic and H-loss fragments of $HFe_4(CO)_{12}(CCH_3)$ were calculated for envelopes corresponding to the loss of 2 to 11 CO ligands resulting in disagreement factors, R, in the 0.06 to 0.11 range. No significant H-loss was seen through the first twelve envelopes. For the parent ion envelope, the value of R was 0.20, which is attributed to the poor signal to noise for these weak peaks. This envelope was one-tenth the intensity of others that were analyzed.

These data clearly establish the general nature of $HFe_4(CO)_{12}(CCH_3)$. In contrast to the species $HFe_4(CO)_{12}(CH)$, which has a butterfly structure, IV, the present compound is tetrahedral, apparently because 3-center bonding which is found in IV and maintains the 62 electron count in that compound, is much less favorable with

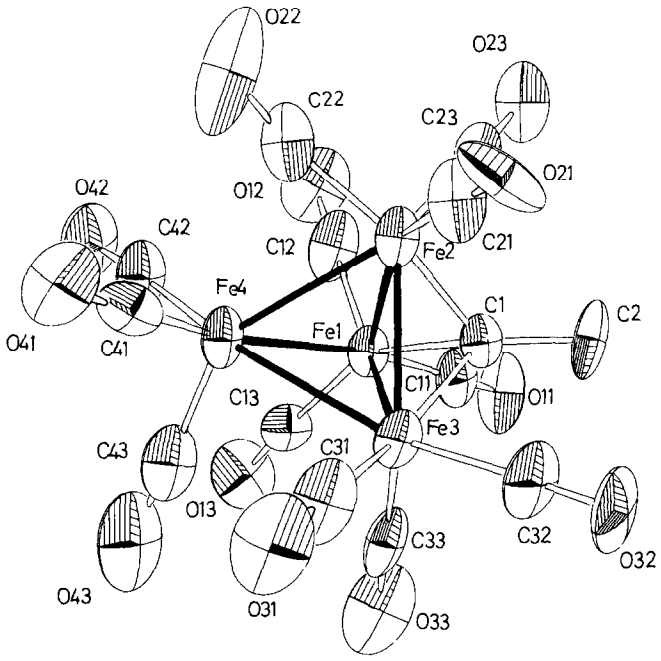

Fig. 1. ORTEP drawing of $HFe_4(CO)_{12}(CCH_3)$. The ethylidyne ligand, CCH_3, appears as C(1) and C(2). A hydride bridge is postulated to occur between Fe(3) and Fe(4).

the ethylidyne ligand and therefore not found in $HFe_4(CO)_{12}(CCH_3)$.

Crystal structure of $HFe_4(CO)_{12}(CCH_3)$. This compound crystallizes in a trigonal unit cell $P3_221$ with one cluster per asymmetric unit. The 60 electron cluster displays the expected tetrahedral arrangement of metal atoms with the ethylidyne group bridging one triangular face (Fe–C average 1.946(14) Å) in symmetric fashion (Fe–Fe–C angles 129.3(12)–131.6(9)°), Table 2. Iron–iron distances in the basal plane (2.562(3) Å) are shorter than apical–basal iron distances (average 2.603(3) Å). Similarly, the Fe_{basal}–Fe_{basal} distances are less than the Fe_{basal}–Fe_{apical} distances in the parent anion $[Fe_4(CO)_{12}(CCH_3)]^-$ (2.529(3) and 2.576(2) Å, respectively) [5]. The carbon–carbon distances in the ethylidyne group are similar in the two structures; 1.56(2) Å in the unprotonated cluster, and 1.513(20) Å in the title structure.

TABLE 2

DISTANCES (Å) AND BOND ANGLES (°) FOR $HFe_4(CO)_{12}(CCH_3)$

Fe(1)–Fe(2)	2.548(3)	Fe(1)–Fe(2)–Fe(3)	59.6(1)
Fe(1)–Fe(3)	2.552(3)	Fe(2)–Fe(3)–Fe(1)	59.4(1)
Fe(2)–Fe(3)	2.587(4)	Fe(2)–Fe(1)–Fe(3)	61.0(1)
Fe(1)–Fe(4)	2.585(3)	Fe(1)–Fe(4)–Fe(2)	58.9(1)
Fe(2)–Fe(4)	2.597(4)	Fe(1)–Fe(4)–Fe(3)	58.6(1)
Fe(3)–Fe(4)	2.628(2)	Fe(2)–Fe(4)–Fe(3)	59.3(1)
Fe(1)–C(1)	1.926(12)	Fe(1)–Fe(2)–Fe(4)	60.3(1)
Fe(2)–C(1)	1.929(12)	Fe(3)–Fe(2)–Fe(4)	60.9(1)
Fe(3)–C(1)	1.983(19)	Fe(1)–Fe(3)–Fe(4)	59.9(1)
		Fe(2)–Fe(3)–Fe(4)	59.7(1)
		Fe(2)–Fe(1)–Fe(4)	60.8(1)
C(1)–C(2)	1.513(20)	Fe(3)–Fe(1)–Fe(4)	61.5(1)
		Fe(1)–C(1)–C(2)	131.6(9)
Fe(1)–C(11)	1.847(17)	Fe(2)–C(1)–C(2)	129.3(12)
Fe(1)–C(12)	1.795(18)	Fe(3)–C(1)–C(2)	130.7(11)
Fe(1)–C(13)	1.800(17)		
Fe(2)–C(21)	1.814(13)	Fe(1)–C(11)–O(11)	177.3(13)
Fe(2)–C(22)	1.825(13)	Fe(1)–C(12)–O(12)	176.2(13)
Fe(2)–C(23)	1.800(20)	Fe(1)–C(13)–O(13)	174.1(13)
Fe(3)–C(31)	1.800(20)	Fe(2)–C(21)–O(21)	177.8(14)
Fe(3)–C(32)	1.828(15)	Fe(2)–C(22)–O(22)	170.4(20)
Fe(3)–C(33)	1.777(17)	Fe(2)–C(23)–O(23)	178.5(11)
Fe(4)–C(41)	1.769(15)	Fe(3)–C(31)–O(31)	177.2(18)
Fe(4)–C(42)	1.793(15)	Fe(3)–C(32)–O(32)	177.3(19)
Fe(4)–C(43)	1.775(21)	Fe(3)–C(33)–O(33)	174.5(14)
C(11)–O(11)	1.10(2)	Fe(4)–C(41)–O(41)	177.5(14)
C(12)–O(12)	1.13(2)	Fe(4)–C(42)–O(42)	176.1(21)
C(13)–O(13)	1.15(2)	Fe(4)–C(43)–O(43)	176.3(13)
C(21)–O(21)	1.12(2)		
C(22)–O(22)	1.15(2)		
C(23)–O(23)	1.10(2)		
C(31)–O(31)	1.15(2)		
C(32)–O(32)	1.11(2)		
C(33)–O(33)	1.14(2)		
C(41)–O(41)	1.15(2)		
C(42)–O(42)	1.12(2)		
C(43)–O(43)	1.14(3)		

Proton positions were not evident from a difference Fourier synthesis calculated following the final least-squares cycle. The proton probably bridges apical iron, Fe(4) and basal iron, Fe(3) as evidenced by the lengthening of the Fe(4)–Fe(3) distance (2.628(2) Å). In agreement with this interpretation, the CO ligands are displaced away from the Fe(3)–Fe(4) edge. Protonation of the cluster thus appears to cause little change in the binding of the ethylidyne group or the disposition of the metal framework.

Further reaction of $HFe_4(CO)_{12}(CCH_3)$ with HSO_3CF_3. The infrared spectrum of $HFe_4(CO)_{12}(CCH_3)$ in HSO_3CF_3 displays a broad absorption maximum at 2075 cm^{-1}, which amounts to a shift of 30 cm^{-1} higher frequency from that of the same molecule dissolved in a hydrocarbon solvent and thus indicates the presence of a cationic species, such as $[H_2Fe_4(CO)_{12}(CCH_3)]^+$. This shift is in line with the shift of the principal band from the anion $[Fe_4(CO)_{12}(CCH_3)]^-$, 1980 cm^{-1} to the neutral $HFe_4(CO)_{12}(CCH_3)$, 2045 cm^{-1} and it also parallels the shifts which have been observed in successive protonations of the iron butterfly series [3]. Similarly, the NMR spectrum of this strong acid solution shows two prominent resonances at δ 5.4 and −22.3 ppm, in an intensity ratio of 3/2. These data indicate that protonation has occurred on the metal framework as illustrated in eq. 3. In addition, resonances of minor intensity occur in this solution at δ 0.9, −20.7 and −30.4 ppm, which can be assigned to $[H_2Fe_4(CO)_{12}(CH)]^+$[3], and at −7.5 ppm, which is attributed to $[HFe(CO)_5]^+$ [10].

$$HFe_4(CO)_{12}(CCH_3) + H^+ \rightarrow [H_2Fe_4(CO)_{12}(CCH_3)]^+ \quad (3)$$

The ^1H coupled and decoupled ^{13}C NMR spectra show two signals over the temperature range −30 to +30 °C. The quaternary carbon appears at δ 373 ppm and the terminal carbonyls exhibit a sharp singlet at δ 207 ppm. The freezing point of HSO_3CF_3 places a severe limitation on low temperature NMR experiments, with the result that we could not explore temperatures which were sufficiently low to suppress the fluctional processes. As a result of the apparent fluctionality of the molecule over the accessible temperature range, no conclusions can be drawn from the NMR concerning the disposition of ligands in the product of eq. 3.

The evolution of CO, H_2, CH_4, C_2H_6 and CO_2 is observed on the long-term interaction of $[H_2Fe_4(CO)_{12}(CCH_3)]^+$ with HSO_3CF_3, and several iron-containing products were identified in solution, eq. 4.

$$[H_2Fe_4(CO)_{12}(CCH_3)]^+ + HSO_3CF_3 \rightarrow H_2 + CO + CO_2 + CH_4 + C_2H_6 + [HFe(CO)_5]^+ + [H_2Fe_4(CO)_{12}(CH)]^+ + Fe^{2+} + \ldots \quad (4)$$

The gases were monitored after 7 and 14 days, with the collection of 70% of the total in the first interval. As shown in Table 3 the mole yields of CH_4 and C_2H_6 were very low. The reducing agent, $[Fe_2(CO)_8]^{2-}$, which has been found to eliminate the induction period in the protolysis of $HFe_4(CO)_{12}(CH)$ [3], actually halved the hydrocarbon yield in the present case (Table 3). The production of CH_4 indicates the cleavage of the C–C bond in the ethylidyne ligand and this is further supported by the extraction of $HFe_4(CO)_{12}(CH)$ from the reaction mixture at the end of the experiment. Iron pentacarbonyl also was observed in the pentane extract of the neutralized reaction mixture.

TABLE 3

GAS EVOLUTION DATA

Gas	Moles per mole of cluster		
	7 days	14 days	7 days [a]
H_2	1 20	1.23	0.51
CO	2.43	3.87	1.47
CH_4	0.03	0.03	0.02
C_2H_6	0.08	0.09	0.06
CO_2	0.01	0.01	0.25

[a] With added reducing agent: 0.4 moles $[Fe_2(CO)_8]^{2-}$ per mole of $[Fe_4(CO)_{12}(CCH_3)]$

In DSO_3CF_3 the sole two-carbon protolysis product, as judged by mass spectroscopy, was $C_2H_3D_3$. The fragmentation pattern of this product revealed the successive loss of HD [11]. This result indicates that the $C_2H_3D_3$ should be formulated as CH_3CD_3 because the favored fragmentation process in ethane is loss of dihydrogen from adjacent carbon atoms. By contrast, the methane which was produced is a mixture of all of the deuterated species, with CD_4 and CD_3H making up approximately 75% of the products. Only approximately 5% of the total is CH_3D. These data indicate that the processes for ethane evolution are quite different from those for methane.

Judging from the observation of CH_3CD_3 as the C_2 product it appears that the protolysis leading to this product occurs by a simple cleavage of the Fe–C bonds between the α-carbon of the ethylidyne and the attached three iron atoms. It is attractive to postulate that this process occurs by the protonation of the metal framework followed by reductive elimination of a Fe–C bond, as has been inferred from a number of studies of reductive elimination reactions [12–16]. One possible course which this set of reductive eliminations might take is given in Scheme 1.

The cleavage of the ethylidyne to produce methane and the methylidyne cluster $HFe_4(CO)_{12}(CH)$ is more difficult to rationalize than the production of ethane. The ethylidyne ligand may be activated toward cleavage by bonding to the 3-iron triangle which may stabilize species such as an acylium, VIII, in eq. 5.

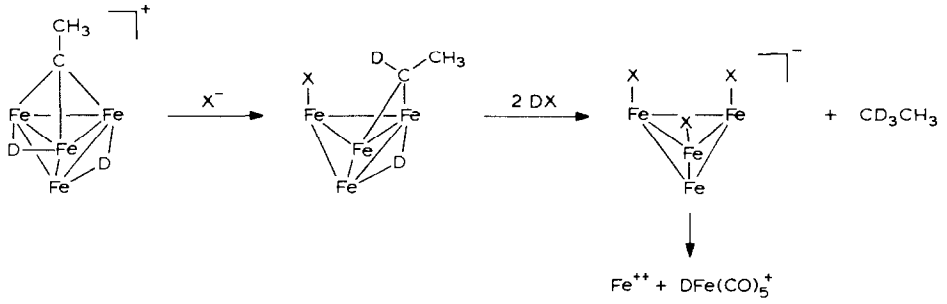

SCHEME 1

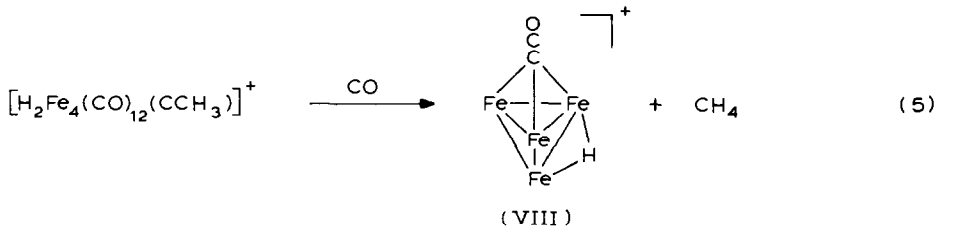

(VIII)

Acknowledgments

This research was supported by the NSF through Grants CHE-7918010 and CHE-8204401. P.L.B. thanks the NSF for a Graduate Fellowship. We thank Prof. H.D. Kaesz for a copy of program MASPAN.

References

1 K. Whitmire and D.F. Shriver, J. Am. Chem. Soc., 102 (1980) 1456.
2 E.M. Holt, K.H. Whitmire, and D.F. Shriver, J. Organomet. Chem., 213 (1981) 125.
3 M.A. Drezdzon and D.F. Shriver, J. Mol. Catal., 21 (1983) 81.
4 M. Monassero, M. Sansoni and G. Longoni, J. Chem. Soc. Chem. Commun., (1976) 919.
5 E.M. Holt, K.H. Whitmire, and D.F. Shriver, J. Am. Chem. Soc., 104 (1982) 5621.
6 K.H. Whitmire, J. Ross, C.B. Cooper III, and D.F. Shriver, Inorg. Synth., 21 (1982) 66.
7 J.M. Stewart, Ed. The XRAY System System Version of 1980, Technical Report TR446 of the Computer Center, University of Maryland, College Park, Maryland.
8 D.T. Cromer and I.B. Mann, Acta Cryst., A, 24 (1968) 321.
9 K. Wade, Adv. Inorg. Chem. Radiochem., 18, (1976) 67; D.M.P. Mingos, Nature (London), Phys. Sci., 236 (1972) 99; J.W. Lauher, J. Am. Chem. Soc., 100 (1978) 5305.
10 A. Davison, W. McFarlane, L. Pratt, and G. Wilkinson, J. Chem. Soc., (1962) 3653.
11 Relative abundances: $m/e = 33$, 35.9; 32, 61.2; 31, 20.5; 30, 100.0; 29, 22.0. Peak at $m/e = 32$ is due in part to O_2.
12 R.W. Johnson and R.G. Pearson, Inorg. Chem., 10 (1971) 2091.
13 M.D. Johnson, Accounts Chem. Res., 11 (1978) 57.
14 J.R. Norton, Accounts Chem. Res., 12 (1979) 139.
15 M.B. Hursthouse, R.A. Jones, K.M. Abdul Malik, and G. Wilkinson, J. Am. Chem. Soc., 101 (1979) 4128.
16 W.A. Herrmann, Adv. Organomet. Chem., 20 (1982) 159.